2023 62nd IEEE Conference on Decision and Control (CDC)
December 13-15, 2023. Marina Bay Sands, Singapore

Early Intention Prediction of Lane-Changing Based on Dual Gaussian-Mixed Hidden Markov Models

Zheng Li, Yijing Wang, Zhiqiang Zuo, Zhengxuan Liu, Yining Chen and Hongchao Li

Abstract— **Adjacent lane-changing is one of the most dangerous maneuvers which may lead to rear-end crash, uncomfortable braking and sharp steering. If the autonomous driving system can predict the potential latent lane-changing intentions of surrounding vehicles in advance, the driver will have more time to make reasonable response. In this paper, we focus on how to give accurate and reliable prediction for latent lane-changings, especially before the vehicles merge into the target lanes. A prediction model based on dual Gaussian-mixed hidden Markov models is developed to exploit the advantages of different features more effectively. Since there is no comprehensive criteria to evaluate the accuracy and predictability performance simultaneously, we propose two new metrics for quantitative analysis as supplement to the classical indicators. Comparative validation on Next Generation Simulation (NGSIM) database shows that our model has a high recognition accuracy of 93.05% for lane-changing intention with earlier prediction over the existing homologous methods.**

I. Introduction

Inspired by the unmanned mobile robots, a classical framework for autonomous vehicles has been proposed, which consists of perception layer, planning layer and control layer [1], [2]. Nevertheless, scholars have realized that for autonomous driving system, it is difficult for planner to directly use the information detected by sensors for robust trajectory generation. This is caused by flexible mobility, non-negligible disturbance and personalized style of surrounding vehicles, especially in complex traffic flows. Therefore, macroscopic intention prediction is necessary for motion decision in autonomous driving. It operates after the perception function but before the planning function [3], [4].

In all traffic scenarios, lane changing is one of the most dangerous maneuvers. It occurs at intersections, on-ramps or off-ramps, and discretionarily during overtaking on highways. It is known that about 40% of crashes are caused by inappropriate lane changing, including not using turn signals, not checking rear-view mirrors or aggressive steering [5]–[7]. To this end, a lot of research has been conducted on intention recognition for lane changing maneuvers [8]–[11]. The past few years have witnessed several backbone models, including support vector machine (SVM) [12], [13], fuzzy inference system (FIS) [14], [15], Bayesian network (BN) [16], hidden Markov model (HMM) [17]–[19] and long short-term memory (LSTM) [20]–[22] and so on. Balbal *et al*. [14] collected the first moment of lateral velocity of not less than 0.2m/s as the lane changing saliency and recognized the maneuvers with a 51-rules-based FIS. Li *et al*. [16] combined Bayesian network with Gaussian-mixed model (GMM) for better accuracy. It is worth noting that the HMM-based models have been widely used in recognition and prediction tasks. Xia *et al*. [18] proposed a human-like intention understanding model in terms of HMM to achieve reliable prediction four seconds before the merging moment. Sharma *et al*. [19] integrated continuous and discrete HMMs to develop an early behavior predictor. However, there are still several key issues that have not been well studied, for example, feature collection, pipeline design, evaluation metrics, etc.

In this work, a novel intention prediction scheme is designed to realize early warning of lane changing maneuvers. It is implemented based on dual GM-HMM pipes, where different features are handled separately. A linear comparator is developed to fuse the output probabilities of dual pipes and determine the most likely maneuver of the target vehicle. With the help of our proposed scheme, the advantages of different features can be independently enhanced at different prediction stages. Furthermore, two comprehensive metrics which simultaneously involve predictability and validity are proposed. Comparative experiments on public dataset demonstrate that our predictor can achieve more satisfactory performance than other homologous methods. The main contributions are two-fold:

- An intention prediction model is developed to realize early lane changing recognition. Two separate GM-HMM pipes are designed to take full advantage of different features. Comparative evaluation shows that our method has higher sensitivity on lane changing intentions.
- Two new evaluation metrics are proposed for comprehensively evaluating both validity and predictability. Using the new metrics, the performance of prediction models can be enhanced by involving both lane changing and lane keeping intentions.

This work was supported by National Natural Science Foundation of China (grants 62173243, 61933014), Tianjin Municipal Science and Technology Project (grant 17ZXRGGX00140) and Tianjin Research Innovation Project for Postgraduate Students (grant 2021YJSO2B09).

Zheng Li, Yijing Wang, Zhiqiang Zuo and Zhengxuan Liu are with the Tianjin Key Laboratory of Intelligent Unmanned Swarm Technology and System, School of Electrical and Information Engineering, Tianjin University, Tianjin 300072, China. {zhengl, yjwang, zqzuo, liuzhengxuan}@tju.edu.cn

Yining Chen is with the School of Artificial Intelligence, Tiangong University, Tianjin 300387, China. chenyining@tiangong.edu.cn

Hongchao Li is with the School of Artificial Intelligence, Hebei University of Technology, 300401, China. hcli@hebut.edu.cn

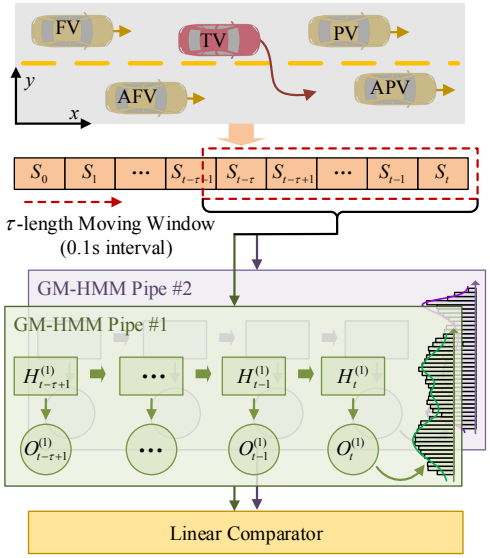

Fig. 1. The intention predictor for latent lane changing maneuvers with dual GM-HMM pipes.

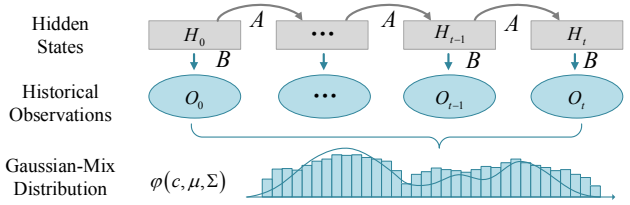

Fig. 2. A single GM-HMM pipe for intention prediction.

II. Methodology

A. Architecture

The overall pipeline is illustrated in Fig. 1. The red vehicle is the target vehicle (TV) which may perform lane changing and the yellow vehicles are the surrounding ones that have a significant impact on the driving of TV. They are the preceding vehicle (PV), the following vehicle (FV), the preceding vehicle in the adjacent lane (APV) and the following vehicle in the adjacent lane (AFV). It is noted that in this work, we address the scenario that a left lane changing and a right one are symmetric and can be modeled by a unified intention predictor. Therefore, only the vehicles traveling on adjacent lanes that are merged by TV are considered in one prediction.

At the current time t, a moving window with length τ is utilized to capture the historical states within 0.1 second interval. If $t-\tau<0$, all the previous states from the initial time $t=0$ to time t are reserved. Otherwise, only the latest τ frames of states are collected. The historical states are then input into the dual GM-HMM pipes to separately generate the maneuver probabilities. Finally, a linear comparator is introduced to determine whether the current driving intention of TV is lane changing or lane keeping. Compared with the existing models, the remarkable difference lies in the introduction of dual pipes to realize the recognition task with different features. The detailed process will be described in the following subsections.

B. Single GM-HMM Pipe

As mentioned above, there are two GM-HMM pipes in our intention predictor. For convenience, we first explain the principle of a single GM-HMM pipe in Fig. 2. Given a hidden state set $\{H_1, H_2, ..., H_{N_h}\}$ where N_h is the number of hidden states, the GM-HMM pipe can be characterized by $\mathcal{M}(\boldsymbol{\pi_0}, \boldsymbol{A}, \boldsymbol{\Phi})$. Here $\boldsymbol{\pi_0}$ indicates the initial probability vector and $\boldsymbol{A}$ is the transition matrix. $\boldsymbol{\Phi}=\{\varphi_1, \varphi_2, ..., \varphi_{N_h}\}$ represents a list of probability density functions and each $\varphi_i, i=1,2,...,N_h$ reflects a Gaussian-mixed distribution with N_m centers. More specific,

$$\mathcal{M}(\boldsymbol{\pi_0}, \boldsymbol{A}, \boldsymbol{\Phi}),\ \boldsymbol{\Phi}=\{\varphi_1, \varphi_2, ..., \varphi_{N_h}\} \tag{1a}$$

$$\boldsymbol{\pi_0}=[\pi_{0i}]\in\mathbb{R}^{N_h},\ \pi_{0i}=P\left(H_0=H_i\right) \tag{1b}$$

$$\boldsymbol{A}=[a_{ij}]\in\mathbb{R}^{N_h\times N_h},\ a_{ij}=P\left(H_{t+1}=H_j|H_t=H_i\right) \tag{1c}$$

$$b_i(O_t)=P\left(O_t|H_t=H_i\right)=\int_{-\infty}^{O_t}\varphi_i(\boldsymbol{\zeta})\mathrm{d}\boldsymbol{\zeta} \tag{1d}$$

$$\begin{aligned}\varphi_i(\boldsymbol{\zeta}) &= \varphi_i(\boldsymbol{\zeta}|\boldsymbol{c}_i, \boldsymbol{\mu}_{i,1}, ..., \boldsymbol{\mu}_{i,N_m}, \boldsymbol{\Sigma}_{i,1}, ..., \boldsymbol{\Sigma}_{i,N_m}) \\ &= \sum_{j=1}^{N_m} c_{i,j}\frac{\exp\left(-\frac{1}{2}\left(\boldsymbol{\zeta}-\boldsymbol{\mu}_{i,j}\right)^{\mathrm{T}}\boldsymbol{\Sigma}_{i,j}^{-1}\left(\boldsymbol{\zeta}-\boldsymbol{\mu}_{i,j}\right)\right)}{\sqrt{(2\pi)^M}\sqrt{|\boldsymbol{\Sigma}_{i,j}|}}\end{aligned} \tag{1e}$$

The element a_{ij} indicates the conditional probability of the next hidden state $H_{t+1}=H_j$ with respect to the current one H_i. Similarly, $b_i(O_t)$ stands for the output probability of generating the observation O_t based on the hidden state H_i, which is determined by the distribution with φ_i. $\boldsymbol{c}_i=[c_{i,1}, ..., c_{i,N_m}]$ is the weight coefficient vector, $\boldsymbol{\mu}_{i,j}$ stands for the mean vector and $\boldsymbol{\Sigma}_{i,j}$ represents the corresponding covariance. M is the dimensional size of the observation O_t.

At time t, the historical observations are collected as $\mathcal{O}_{0:t}=\{O_0, O_1, ..., O_t\}$, and the probability of obtaining $\mathcal{O}_{0:t}$ under model $\mathcal{M}(\boldsymbol{\pi_0}, \boldsymbol{A}, \boldsymbol{\Phi})$ can be determined by

$$P(\mathcal{O}_{0:t}|\mathcal{M})=\sum_{i=1}^{N_h}P(H_t=H_i|\mathcal{M}) \tag{2a}$$

$$P(H_t=H_i|\mathcal{M})=b_i(O_t)\Big[\sum_{i=1}^{N_h}a_{ji}P(H_{t-1}=H_j|\mathcal{M})\Big] \tag{2b}$$

$$P(H_0=H_i|\mathcal{M})=\pi_{0i}b_i(O_0) \tag{2c}$$

It is noted that in a single GM-HMM pipe, there are always two independent models, i.e, $\mathcal{M}_{\mathrm{LC}}$ designed for lane changing maneuver and $\mathcal{M}_{\mathrm{LK}}$ for lane keeping maneuver. This is consistent with the previous studies [10], [11], [18]. And the output driving intention can be finally characterized by a ratio form with respect to a certain threshold $\varepsilon_{\mathrm{LC}}$, that is,

$$\varepsilon:=\frac{P(\mathcal{O}_t|\mathcal{M}_{\mathrm{LC}})}{P(\mathcal{O}_t|\mathcal{M}_{\mathrm{LK}})}>\varepsilon_{\mathrm{LC}} \tag{3}$$

where variable ε is defined as the ratio between the probability of lane changing and that of lane keeping for two models.

C. Feature with Dual Pipes

As shown in Fig. 1, there are dual pipes to separately process the input historical states, where different features are extracted from different pipes. More specific,

$$\begin{cases} O_t^{(1)} = [\Delta x_*, \Delta v_*^x], \\ O_t^{(2)} = [v_{\mathrm{TV}}^y, \psi_{\mathrm{TV}}, TTC_*^{inv}] \\ * \in \{\mathrm{PV}, \mathrm{FV}, \mathrm{APV}, \mathrm{AFV}\} \end{cases} \tag{4}$$

where v_{TV}^y and ψ_{TV} are respectively the lateral velocity of the target vehicle TV and its heading. TTC_*^{inv} represents the inverse of time-to-collision with respect to vehicle $*$. Δx_* and Δv_*^x indicate the relative longitudinal distance and relative longitudinal velocity between vehicle $*$ and TV.

Remark 1: As pointed out in [18], there are various features that describe the driving maneuvers at different stages of lane changing. The lateral features such as position offset and lateral velocity are significant ones characterizing the instant of changing lanes. While in contrast, at the early stage of lane changing, the longitudinal velocity of TV will fluctuate to ensure a safe distance from vehicles in front and behind. Therefore, the relative longitudinal information in $O_t^{(1)}$ is regarded as a useful indication of lane changing in [11], [18]. Since two kinds of features in (4) are collected to characterize the maneuvers of TV at different stages, we tackle them with two separate pipes to avoid possible conflicts between different features.

A τ-length observation sequence with the i-th feature can be written as $\mathcal{O}_{t-\tau+1:t}^{(i)} = \{O_{t-\tau+1}^{(i)}, ..., O_t^{(i)}\}$. Then $\mathcal{O}_{t-\tau+1:t}^{(i)}$ will be used to obtain the probability ratio $\varepsilon^{(i)}$ through the i-th GM-HMM pipe. The detailed pipeline has been explained in the previous subsection.

D. Linear Comparator

Unlike the widely used comparator in previous studies in (3), our method uses a linear comparator since there are two output probability ratios $\varepsilon^{(1)}$ and $\varepsilon^{(2)}$ generated by the dual pipes. It is formulated as

$$I_{\mathrm{LC}} = \begin{cases} 1, & \text{if } \alpha_1 \varepsilon^{(1)} + \alpha_2 \varepsilon^{(2)} > \varepsilon_{\mathrm{LC}} \\ 0, & \text{otherwise} \end{cases} \tag{5}$$

where α_1 and α_2 are weight coefficients and $\varepsilon_{\mathrm{LC}}$ is the threshold. $I_{\mathrm{LC}} = 1$ indicates that the driving intention is lane changing.

E. Implementation

Table I lists the parameters for our intention prediction model. The model is constructed with third-party tools including sklearn and hmmlearn. The dual GM-HMM pipes in our predictor are independently trained through Baum-Welch (BW) algorithm. At the training stage, the model for lane changing and that for lane keeping in a single GM-HMM are separately fitted with labeled data while in the evaluation, the labels of all trajectories are unknown. Furthermore, the moving window with length τ will be utilized to capture observation sequences at each instant. To enhance the training process, cross-validation method is applied to obtain the best trained model.

TABLE I
MODEL PARAMETERS.

Parameter	Variable	Value
Number of hidden states	N_h	3
Number of Gaussian-mixed center	N_m	3
Weights in linear comparison	(α_1, α_2)	(0.81, 1.64)
Threshold of lane changing	$\varepsilon_{\mathrm{LC}}$	0.31
Observation length	τ	{1s, 3s}

III. Data and Metrics

A. Data Collection

In this work, all the trajectories used for training and evaluation are collected from the US-101 and I-80 datasets in NGSIM. And some necessary rules are implemented during pre-process as follows.

- The trajectories in lanes 1 to 6 are collected where the mandatory and discretionary lane changing maneuvers are involved.
- A lane changing trajectory longer than 1 second is collected and its historical observations for 7 seconds before crossing the lane mark will be reserved.
- There are some situations where lane changing fails. More specific, TV crossed the lane mark but immediately returned to its original lane as shown in Fig. 3. These trajectories are removed since it is unreasonable to classify them as lane changing or lane keeping.

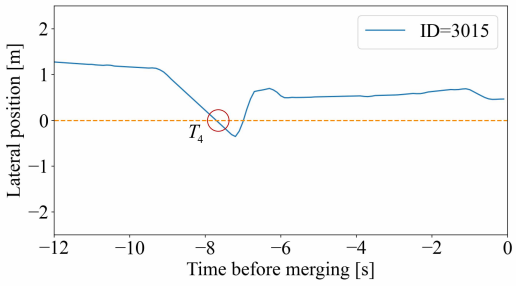

Fig. 3. A failed lane changing.

With the above criteria, 2341 lane changing trajectories and 3570 lane keeping ones are ultimately selected from the dataset. A statistical data for lane changing trajectories is given in Fig. 4. From the histogram it can be found that more than 33% (787 in total) drivers complete the lane changing process in less than 4 seconds. And more than 6% (147 in total) trajectories are even shorter than 2 seconds. They belong to aggressive maneuvers which pose a significant collision risk to the following vehicles. This indicates that an early intention prediction is crucial for warning vehicles behind to slow down and keep a safe distance.

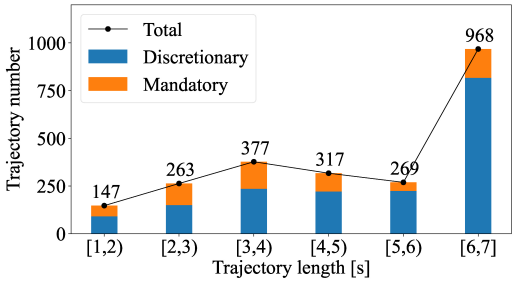

Fig. 4. Statistics of lane changing trajectories.

Finally, 60% of the samples are randomly split into the training set, and the others are used for evaluation. For a lane changing trajectory, if it can be identified immediately before crossing the lane mark, it is categorized as a true positive sample, otherwise a false negative one. In contrast, for a lane keeping trajectory, it will only be marked as a true negative sample if there is no false alarm throughout the time span.

B. Evaluation Metrics

The well known metrics for evaluating intention prediction include sensitivity, specificity, recall, precision and F_1-score. Their detailed definitions are given below.

$$\text{Sensitivity} = \text{Recall} = \frac{\text{TP}}{\text{TP} + \text{FN}} \tag{6a}$$

$$\text{Specificity} = \frac{\text{TN}}{\text{TN} + \text{FP}} \tag{6b}$$

$$\text{Precision} = \frac{\text{TP}}{\text{TP} + \text{FP}} \tag{6c}$$

$$F_1\text{-Score} = \frac{2 \times \text{Recall} \times \text{Precision}}{\text{Recall} + \text{Precision}} \tag{6d}$$

In addition, the receiver operating characteristic (ROC) curve and the area under curve (AUC) are adopted to analyze the relationship between TP rate and FP rate. They are important indicators that reflect the comprehensive performance of models. A ROC curve with higher AUC value indicates that the model has better classification ability.

However, there is a flaw in the above metrics, that is, they only reflect the prediction validity at a specific instant. In most existing studies, only the predicted intentions at a single instant are employed for evaluation. While in terms of practical applications, not only the validity at lane changing instants but also the predictability (how early the lane changing intention can be recognized) should be involved to comprehensively assess the performance.

Remark 2: To analyze the effectiveness of intention prediction models at various instants, some attempts have been made in previous literature and several indicators have been proposed, for example, recall-time curve [18], [19], [22], recognition rate [17] and prediction time [23], [24]. It is known that these indicators cannot comprehensively characterize the prediction performance of both lane changing and lane keeping maneuvers. Furthermore, variable length trajectories should be included in the evaluation.

Motivated by the above discussions, we design two new metrics, namely, average recall of forewarning (ARoF) and F_β-ARoF. ARoF is defined as the area under the recall of prediction (RoF) curve

$$\text{ARoF} = \frac{1}{|T_{\max}|} \int_{T_{\max}}^{0} \text{RoF}(t) \mathrm{d}t \tag{7a}$$

$$\text{RoF}(t) = \frac{\text{TP}(t_r < t)}{num_{|t|}} \tag{7b}$$

where $T_{\max}$ indicates the earliest instant determined by the maximum length of all trajectories. t_r stands for the moment when the lane changing intention is successfully identified, and $\text{TP}(t_r < t)$ represents the number of true-positive samples before time t. It is noted that the denominator $num_{|t|}$ is the number of trajectories with a length greater than $|t|$. Since there is no fixed length of lane changing trajectories in our study, $num_{|t|}$ will be specified variably at different instants. In terms of practical calculation, the integration in (7) can be approximated by

$$\text{ARoF} \approx \frac{1}{L+1} \sum_{k=0}^{L} \text{RoF}\left(\frac{k}{L} T_{\max}\right)$$

with L being the number of sampling instants. Fig. 5 plots the RoF curve and the ratio of gray area to time-span (length of the horizontal axis) is ARoF.

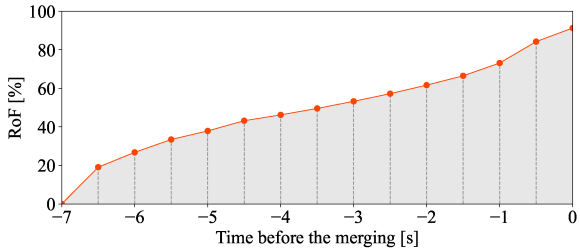

Fig. 5. Illustration of the RoF curve and ARoF.

It should be emphasized that ARoF actually characterizes the average prediction correction of lane changing maneuvers over the entire time-span, while the false alarm is not addressed for real lane keeping trajectories. An extreme situation is that an unbelievable predictor asserting all trajectories as lane changing ones can still achieve 100% ARoF. Therefore, we need a comprehensive indicator to quantify the prediction effectiveness involving both lane changing and lane keeping intentions. Inspired by the concept of F_β-score, we can define F_β-ARoF as

$$F_\beta\text{-ARoF} = (1+\beta^2) \frac{\text{Precision} \times \text{ARoF}}{\beta^2 \times \text{Precision} + \text{ARoF}} \tag{8}$$

where parameter β describes to what extent ARoF is more important than precision. If $\beta > 1$ it means that ARoF plays a crucial role in evaluation, with more emphasis on the prediction correction of lane changing intentions. Otherwise,

TABLE II

RECOGNITION RESULTS ON THE TEST SET.

Observation Length	Methods	Sensitivity ↑	Specificity ↑	AUC ↑	F_1-score ↑	ARoF ↑	F_β-ARoF ↑ $\beta=1$	$\beta=0.5$	$\beta=2$
$\tau=1$s	CHMM-DHMM	53.37%	69.47%	0.6194	53.37%	27.80%	36.56%	45.08%	30.75%
	GM-HMM	73.05%	79.90%	0.8719	71.17%	**46.41%**	55.94%	63.81%	49.80%
	Ours	**93.05%**	**95.80%**	**0.9817**	**93.30%**	46.36%	**62.00%**	**77.73%**	**51.56%**
$\tau=3$s	CHMM-DHMM	53.26%	72.69%	0.6855	54.63%	32.70%	41.31%	49.06%	35.68%
	GM-HMM	72.51%	80.46%	0.8736	71.67%	48.22%	57.38%	64.77%	51.51%
	Ours	**91.87%**	**94.47%**	**0.9842**	**91.72%**	**50.96%**	**65.48%**	**78.99%**	**55.92%**

precision takes a greater weight and false alarm should be eliminated as much as possible.

IV. EVALUATIONS

A. Performance Comparison

In this subsection, we validate the performance on prediction and classification of lane changing and lane keeping maneuvers for our proposed dual-pipe model on the test database. Moreover, we make some comparison with two existing HMM-based methods, that is, GM-HMM in [11] and CHMM-DHMM in [19]. Table II lists the detailed results. To describe the effectiveness of different methods more objectively, we repeat the tests with variable observation lengths where $\tau = 1$s or 3s. From the comparison results, several observations can be summarized in the sequel:

- For the classification metrics, i.e., Sensitivity, Specificity, AUC and F_1-score, it is found that our dual-pipe model outperforms the other two models. The best lane changing recognition sensitivity is higher than 93% and the AUC is up to 0.9842 in our proposed scheme.
- With a shorter observation length of $\tau = 1$s, our model has similar performance on ARoF as GM-HMM in [11], but it is superior to [19]. As the observation length increases, our model can achieve better prediction performance on ARoF. This means that using more historical observations, our scheme can performs well on predictability.
- In terms of the proposed comprehensive metric F_β-ARoF, our scheme has been validated with the highest score wherever τ =1s or 3s. When $\beta = 1$ it means that the predictability (ARoF) and the sensitivity are equally weighted in the evaluation.

For each recognition model, it will output a final score that reflecting the extent that the maneuver is likely to perform lane changing or lane keeping. The ROC curves describe the relationship between TPR and FPR at different thresholds. Fig. 6 plots the ROC curves of three recognizers with different observation lengths. The results are consistent with those in Table II. Note that a ROC curve closer to the lower right indicates worse performance.

B. Ablation Studies

To further analyze the impact of different parts including feature, comparator and observation length, we conduct ablation experiments on the training set.

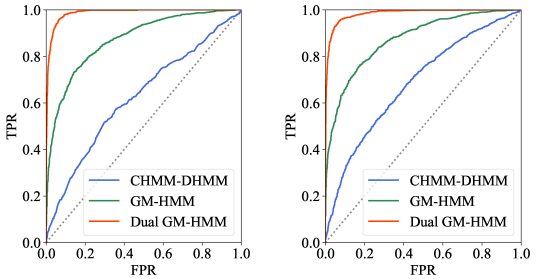

(a) $\tau = 1$s (b) $\tau = 3$s

Fig. 6. ROC curves of three methods, CHMM-DHMM, GM-HMM and our dual model.

1) Feature: To address the effects of different features in our dual-pipe model, the ablation study has been conducted and the results are given in Table III. We can see that our dual-pipe model has more than 12% improvement on F_1-score compared with those that only involve longitudinal feature regardless of the value of τ. And the improvement is up to 3% on ARoF in contrast to those using mixed feature $O_t^{(2)}$. As for the comprehensive metric F_1-ARoF, our model still has at least 3% performance enhancement.

TABLE III

ABLATION TESTS FOR DIFFERENT OBSERVATION FEATURES.

$O_t^{(1)}$	$O_t^{(2)}$	F_1-score ↑	ARoF ↑	F_1-ARoF ↑
✓	×	75.65%	51.14%	61.02%
×	✓	91.15%	47.58%	62.51%
✓	✓	**91.85%**	**51.20%**	**65.76%**

2) Comparator: As mentioned in Section II-D, a linear comparator has been adopted to determine the final output. Here we would like to investigate the effect of comparison forms. Two other forms are the maximum comparator and the Gaussian comparator with formulas as follows.

- *Maximum comparator* with a specific threshold $\varepsilon_{\mathrm{LC}}$ is defined as

$$I_{\mathrm{LC}} = \begin{cases} 1, & \text{if } \max\left\{\varepsilon^{(1)}, \varepsilon^{(2)}\right\} > \varepsilon_{\mathrm{LC}} \\ 0, & \text{otherwise} \end{cases}$$

- *Gaussian comparator* with probability vector $\boldsymbol{\epsilon} = \left[\varepsilon^{(1)}, \varepsilon^{(2)}\right]^{\mathrm{T}}$, mean vector $\boldsymbol{\mu}$ and variance σ^2 can be

expressed as

$$I_{\mathrm{LC}} = \begin{cases} 1, & \text{if } \exp\left\{-\dfrac{\|\boldsymbol{\epsilon}-\boldsymbol{\mu}\|_2^2}{2\sigma^2}\right\} > 0.5 \\ 0, & \text{otherwise} \end{cases}$$

Table IV lists the ablation results with different types of comparators. As for F_1-score, the three comparators have similar effects. However, the linear comparator is a better choice for prediction and comprehensive performance. In summary, the linear comparator has an improvement of about 2% and 1% on the comprehensive metric F_1-ARoF compared to the maximum comparator and the Gaussian one, respectively.

TABLE IV
ABLATION TESTS FOR COMPARATORS.

Comparator	F_1-score ↑	ARoF ↑	F_1-ARoF ↑
Maximum	91.89%	47.71%	62.81%
Gaussian	**92.60%**	50.60%	65.44%
Linear	91.85%	**51.20%**	**65.76%**

V. CONCLUSION

The problem of intention prediction has been investigated in this paper, with the aim of predicting the potential lane changing maneuvers of surrounding vehicles in a mixed traffic flow. First a dual-pipe model based on GM-HMMs has been developed, in which two observation features related to longitudinal and lateral states of surrounding vehicles are collected. These features are respectively utilized in two separate prediction pipes. Compared to other homologous HMM-based methods, our model has been verified with over 13% improvement in prediction sensitivity and specificity. Furthermore, new metrics, ARoF and F_β-ARoF, have been designed to evaluate prediction effectiveness comprehensively. In terms of the new comprehensive metrics, there is at least 5% enhancement by our scheme. Ablation studies have shown that the feature extraction part yields more than 3% improvement and the linear comparator contributes over 1% performance promotion on intention prediction.

VI. REFERENCES

[1] S. Noh and K. An, "Decision-making framework for automated driving in highway environments," *IEEE Transactions on Intelligent Transportation Systems*, vol. 19, no. 1, pp. 58–71, 2018.

[2] L. Claussmann, M. Revilloud, D. Gruyer, and S. Glaser, "A review of motion planning for highway autonomous driving," *IEEE Transactions on Intelligent Transportation Systems*, vol. 21, no. 5, pp. 1826–1848, 2020.

[3] Y. Jeong and K. Yi, "Target vehicle motion prediction-based motion planning framework for autonomous driving in uncontrolled intersections," *IEEE Transactions on Intelligent Transportation Systems*, vol. 22, no. 1, pp. 168–177, 2021.

[4] X. Wang, Y. Guo, C. Bai, Q. Yuan, S. Liu, and J. Han, "Driver's intention identification with the involvement of emotional factors in two-lane roads," *IEEE Transactions on Intelligent Transportation Systems*, vol. 22, no. 11, pp. 6866–6874, 2021.

[5] G. Fitch, S. Lee, S. Klauer, J. Hankey, J. Sudweeks, and T. Dingus, "Analysis of lane-change crashes and near-crashes," *US Department of Transportation, National Highway Traffic Safety Administration*, 2009.

[6] D. Bevly, X. Cao, M. Gordon, G. Ozbilgin, D. Kari, B. Nelson, J. Woodruff, M. Barth, C. Murray, A. Kurt, K. Redmill, and U. Ozguner, "Lane change and merge maneuvers for connected and automated vehicles: A survey," *IEEE Transactions on Intelligent Vehicles*, vol. 1, no. 1, pp. 105–120, 2016.

[7] D. Zhao, H. Lam, H. Peng, S. Bao, D. J. LeBlanc, K. Nobukawa, and C. S. Pan, "Accelerated evaluation of automated vehicles safety in lane-change scenarios based on importance sampling techniques," *IEEE Transactions on Intelligent Transportation Systems*, vol. 18, no. 3, pp. 595–607, 2017.

[8] C. Dong, J. M. Dolan, and B. Litkouhi, "Intention estimation for ramp merging control in autonomous driving," in *2017 IEEE Intelligent Vehicles Symposium (IV)*, 2017, pp. 1584–1589.

[9] Y. Lyu, C. Dong, and J. M. Dolan, "Fg-gmm-based interactive behavior estimation for autonomous driving vehicles in ramp merging control," in *2020 IEEE International Conference on Robotics and Automation (ICRA)*, 2020, pp. 1250–1255.

[10] K. Li, X. Wang, Y. Xu, and J. Wang, "Lane changing intention recognition based on speech recognition models," *Transportation Research Part C: Emerging Technologies*, vol. 69, pp. 497–514, 2016.

[11] H. Jin, C. Duan, Y. Liu, and P. Lu, "Gauss mixture hidden Markov model to characterise and model discretionary lane-change behaviours for autonomous vehicles," *IET Intelligent Transport Systems*, vol. 14, no. 5, pp. 401–411, 2020.

[12] Y. Liu, X. Wang, L. Li, S. Cheng, and Z. Chen, "A novel lane change decision-making model of autonomous vehicle based on support vector machine," *IEEE Access*, vol. 7, pp. 26 543–26 550, 2019.

[13] S. Ramyar, A. Homaifar, A. Karimoddini, and E. Tunstel, "Identification of anomalies in lane change behavior using one-class SVM," in *IEEE International Conference on Systems, Man, and Cybernetics (SMC)*, 2016, pp. 004 405–004 410.

[14] E. Balal, R. L. Cheu, and T. Sarkodie-Gyan, "A binary decision model for discretionary lane changing move based on fuzzy inference system," *Transportation Research Part C: Emerging Technologies*, vol. 67, pp. 47–61, 2016.

[15] J. Tang, F. Liu, W. Zhang, K. Ruimin, and Y. Zou, "Lane-changes prediction based on adaptive fuzzy neural network," *Expert Systems with Applications*, vol. 91, pp. 452–463, 2018.

[16] X. Li, W. Wang, and M. Roetting, "Estimating driverâĂŹs lane-change intent considering driving style and contextual traffic," *IEEE Transactions on Intelligent Transportation Systems*, vol. 20, no. 9, pp. 3258–3271, 2019.

[17] Q. Liu, S. Xu, C. Lu, H. Yao, and H. Chen, "Early recognition of driving intention for lane change based on recurrent hidden semi-Markov model," *IEEE Transactions on Vehicular Technology*, vol. 69, no. 10, pp. 10 545–10 557, 2020.

[18] Y. Xia, Z. Qu, Z. Sun, and Z. Li, "A human-like model to understand surrounding vehicles' lane changing intentions for autonomous driving," *IEEE Transactions on Vehicular Technology*, vol. 70, no. 5, pp. 4178–4189, 2021.

[19] O. Sharma, N. C. Sahoo, and N. B. Puhan, "Highway discretionary lane changing behavior recognition using continuous and discrete hidden Markov model," in *IEEE International Conference on Intelligent Transportation Systems (ITSC)*, 2021, pp. 1476–1481.

[20] D. Xie, Z. Fang, B. Jia, and Z. He, "A data-driven lane-changing model based on deep learning," *Transportation Research Part C: Emerging Technologies*, vol. 106, pp. 41–60, 2019.

[21] Q. Zou, Y. Hou, and Z. Wang, "Predicting vehicle lane-changing behavior with awareness of surrounding vehicles using LSTM network," in *IEEE International Conference on Cloud Computing and Intelligence Systems (CCIS)*, 2019, pp. 79–83.

[22] L. Xin, P. Wang, C. Chan, J. Chen, S. Li, and B. Chen, "Intention-aware long horizon trajectory prediction of surrounding vehicles using dual LSTM networks," in *IEEE International Conference on Intelligent Transportation Systems (ITSC)*, 2018, pp. 1441–1446.

[23] F. WirthmÃijller, J. Schlechtriemen, J. Hipp, and M. Reichert, "Teaching vehicles to anticipate: A systematic study on probabilistic behavior prediction using large data sets," *IEEE Transactions on Intelligent Transportation Systems*, vol. 22, no. 11, pp. 7129–7144, 2021.

[24] S. Mozaffari, E. Arnold, M. Dianati, and S. Fallah, "Early lane change prediction for automated driving systems using multi-task attention-based convolutional neural networks," *IEEE Transactions on Intelligent Vehicles*, vol. 7, no. 3, pp. 758–770, 2022.